

Supplementary Information

Role of Grain Growth in Controlling the Crystal Orientation of Sb₂S₃ Film for efficient Solar Cell

Chunyan Wu^{a†*}, Lijian Zhang^{bc†}, Bo Che^c, Peng Xiao^c, Junjie Yang^c, Haolin Wang^c, Liang Chu^b, Wensheng Yan^{b*}, and Tao Chen^{c*}

^aLaboratory of Advanced Nano-Optoelectronic Materials and Devices, Ningbo Institute of Materials Technology and Engineering, Chinese Academy of Science, Ningbo, Zhejiang, 315201, People's Republic of China.

^bInstitute of Carbon Neutrality and New Energy, School of Electronics and Information, Hangzhou Dianzi University, Hangzhou, 310018, People's Republic of China.

^cHefei National Research Center for Physical Sciences at the Microscale, CAS Key Laboratory of Materials for Energy Conversion, Department of Materials Science and Engineering, School of Chemistry and Materials Science, University of Science and Technology of China, Hefei, Anhui, 230026, People's Republic of China.

These authors contributed equally to this work

*Corresponding Authors:

E-mail: wuchunyan@nimte.ac.cn; wensheng.yan@hdu.edu.cn; tchenmse@ustc.edu.cn

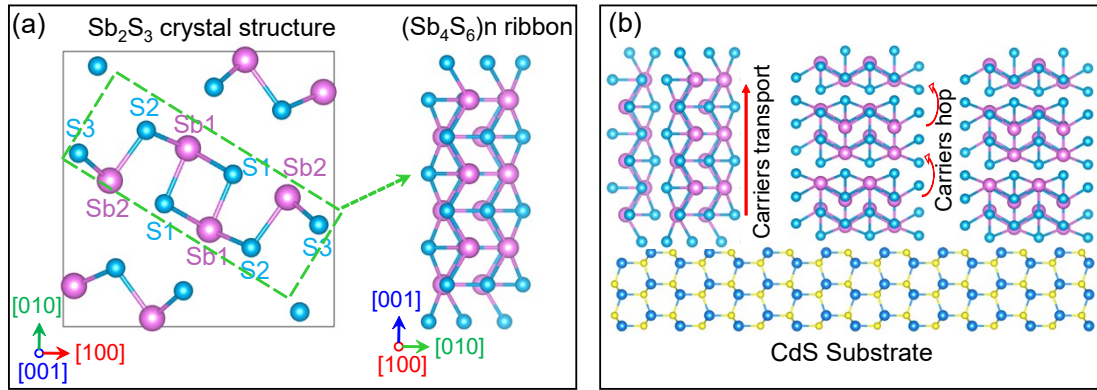


Figure S1. (a) The crystal structure of Sb_2S_3 and $(\text{S}_4\text{S}_6)_n$ ribbon. (b) Schematic diagram showing the photogenerated carriers transport in solar cell with horizontally- $[\text{hk}0]$ or vertically- $[\text{hk}1]$ oriented Sb_2S_3 .

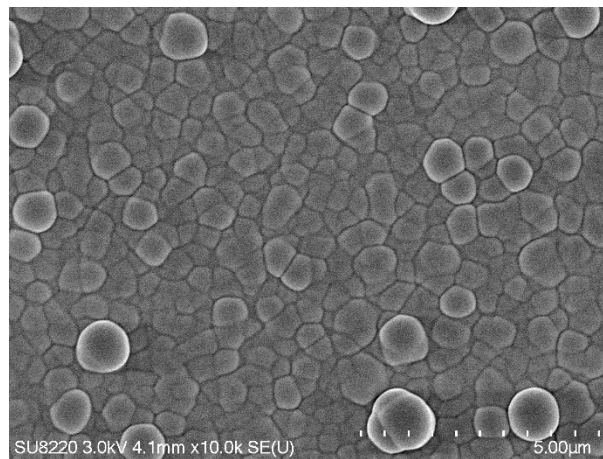


Figure S2. SEM surface image of the precursor Sb_2S_3 film without annealing treatment.

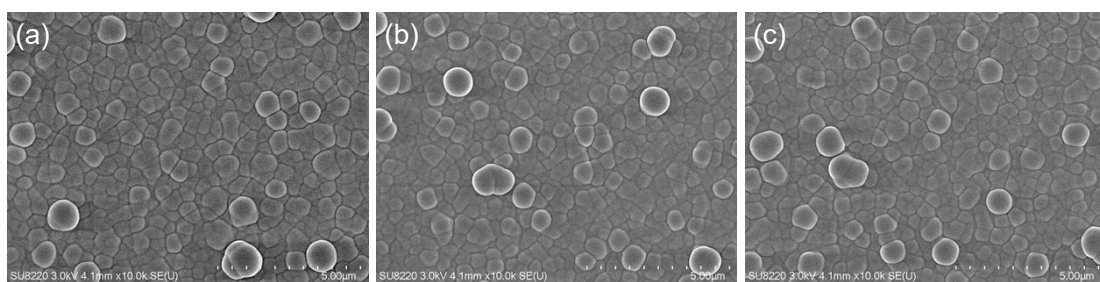


Figure S3. SEM surface images of Sb_2S_3 were removed from the hotplate at the temperature of (a) 150 $^\circ\text{C}$, (b) 200 $^\circ\text{C}$, and (c) 250 $^\circ\text{C}$.

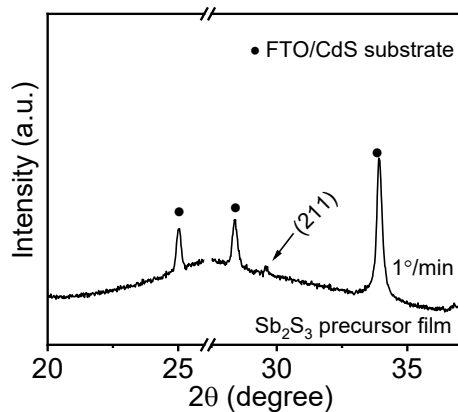


Figure S4. The XRD pattern of the precursor Sb_2S_3 film with the XRD measurement at the scan speed of $1^\circ/\text{min}$.

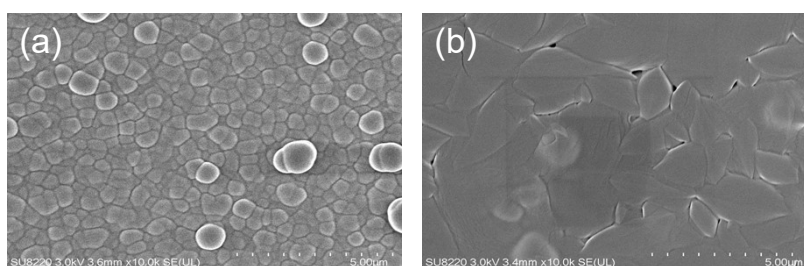


Figure S5. SEM surface images of the precursor Sb_2S_3 was directly annealed at 300°C for (a) 10 S and (b) 20 S.

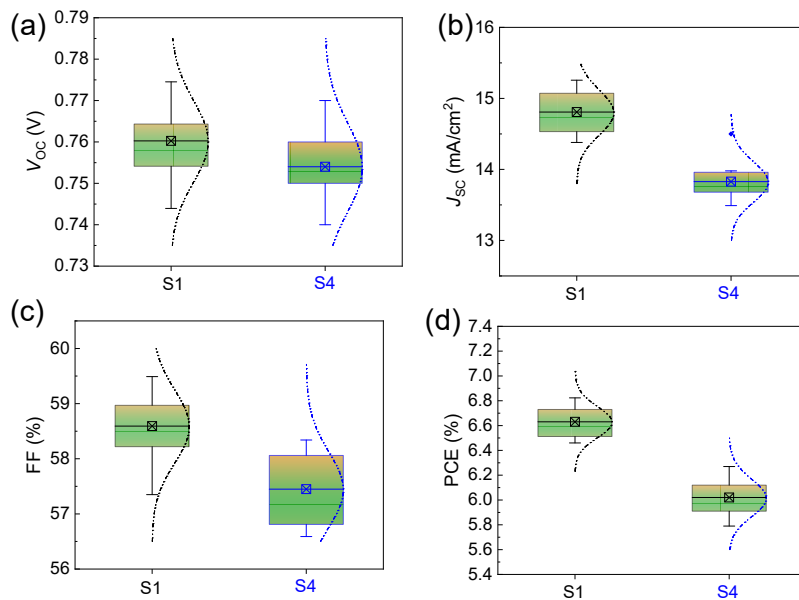


Figure S6. Statistic parameters of (a) V_{oc} , (b) J_{sc} , (c) FF, and (d) PCE obtained from 10 devices based on S1 and S4 films.

Table S1. Texture ecoefficiency of (120), (220), (130), (211), and (221) for each sample.

\square	S1	S2	S3	S4
$\square(120)$	0.638604	0.686054	0.950391	1.136597
$\square(220)$	0.914345	0.903854	1.423648	1.722235
$\square(130)$	0.739076	0.742605	0.787764	0.954708
$\square(211)$	1.431874	1.444875	0.94301	0.532435
$\square(221)$	1.272573	1.226141	0.895186	0.654025

Table S2. The detail parameters of the biexponential fitting of TAS decay.

Sample	A_1	t_1 (ps)	A_2	t_2 (ps)	t_{ave} (ps)
S1	0.26	180	0.74	3984	3924
S4	0.15	239	0.85	4858	4818

Table S3. The trap energy level (E_T), cross section (σ), level deep defect concentration (N_T), and defect type in S1 and S4 films.

Sample	level	E_V (eV)	Sigma (cm^2)	N_T (cm^{-3})	
S1	H2	$E_V+0.702$	$2.21*10^{-15}$	$1.42*10^{14}$	S_{sb}
S4	H1	$E_V+0.576$	$2.52*10^{-17}$	$6.67*10^{13}$	V_{sb}
	H2	$E_V+0.701$	$4.37*10^{-16}$	$1.08*10^{14}$	S_{sb}

Note S1: Background of DLTS measurement ^[1]

Here we conducted deep-level transient spectroscopy (DLTS) to detect the defect

properties. The activation energy (E_a) as well as capture cross-section(σ) of defects can be calculated from Arrhenius plots based on the following equations:

$$\ln(\tau_e v_{th,n} N_C) = \frac{E_C - E_T}{k_B T} - \ln(X_n \sigma_n) \quad (1)$$

$$\ln(\tau_e v_{th,p} N_V) = \frac{E_T - E_V}{k_B T} - \ln(X_p \sigma_p) \quad (2)$$

where τ_e represents the emission time constant, $v_{th,n}$ and $v_{th,p}$ are the thermal velocities associated with electron and hole traps, N_C and N_V are the effective densities of states of conduction (E_C) and valence(E_V) bands, X_n and X_p are the entropy factor of hole and electron, σ_n and σ_p represent the capture cross-section of electron and hole traps, respectively. T and k_B are the temperature and Boltzmann constant, respectively. E_T is the energy level of defect. Additionally, $v_{th,n}$ and N_C can be obtained from equation (3) and (4):

$$v_{th,n} = \sqrt{\frac{3k_B T}{m_n^*}} \quad (3)$$

$$N_c = 2 \left(\frac{2\pi m_n^* k_B T}{h^2} \right)^{\frac{3}{2}} \quad (4)$$

where m_n^* is the effective mass for electrons, with similar equations for $v_{th,p}$ and N_V . We obtain the activation energy of electron ($E_C - E_T$) and hole ($E_T - E_V$) traps from the slope of equations (1) and (2) through linear regression. The σ_p and σ_n values can be extracted from the intersection of line with y-axis. The trap concentration (N_T) can be obtained from equation (5):

$$N_T = 2N_S \frac{\Delta C}{C_R} \quad (5)$$

N_T is the trap concentration. N_S represents the shallow dopant concentration in the films. C_R and ΔC represent the capacitance at reverse bias in equilibrium and the amplitude of capacitance transient, respectively.

Reference

[1] R. Tang, X. Wang, W. Lian, J. Huang, Q. Wei, M. Huang, Y. Yin, C. Jiang, S. Yang, G. Xing, S. Chen, C. Zhu, X. Hao, M. A. Green, T. Chen, *Nat. Energy* **2020**, *5*, 587.